

# C–H Cleavages in the Photoreactions of $[M_2(\eta^5\text{-C}_5\text{H}_5)_2(\text{CO})_6]$ (M = Mo, W): Isolation and Characterization of the V-Shaped Trinuclear Clusters $[M_2M'(\mu\text{-}\eta^1, \eta^5\text{-C}_5\text{H}_4)(\eta^5\text{-C}_5\text{H}_5)_2(\text{CO})_6]$ (M, M' = Mo or W)

M. Angeles Alvarez,<sup>†</sup> M. Esther García,<sup>†</sup> Víctor Riera,<sup>\*,†</sup> Miguel A. Ruiz,<sup>†</sup> Claudette Bois,<sup>‡</sup> and Y. Jeannin<sup>‡</sup>

Contribution from the Instituto de Química Organometálica, Universidad de Oviedo, 33071 Oviedo, Spain, and Laboratoire de Chimie des Métaux de Transition, UACNRS 419, Université P. et M. Curie, 4 Place Jussieu, 75252 Paris, Cedex 05, France

Received August 29, 1994<sup>⊗</sup>

**Abstract:** Irradiation of toluene solutions of the complexes  $[M_2\text{Cp}_2(\text{CO})_6]$  (M = Mo, W; Cp =  $\eta^5\text{-C}_5\text{H}_5$ ) with UV–visible light at  $-35^\circ\text{C}$  gives the new trinuclear compounds  $[M_3(\mu\text{-}\eta^1, \eta^5\text{-C}_5\text{H}_4)\text{Cp}_2(\text{CO})_6]$  in moderate (M = Mo) or medium (M = W) yields, along with the known complexes  $[\text{MH}(\text{CO})_3\text{Cp}]$ ,  $[\text{W}_2(\mu\text{-H})_2(\text{CO})_4\text{Cp}_2]$ , and  $[\text{M}_2\text{Cp}_2(\text{CO})_4]$ . Similar treatment of equimolar mixtures of  $[\text{W}_2\text{Cp}_2(\text{CO})_6]$  and  $[\text{Mo}_2\text{Cp}_2(\text{CO})_4]$  gives a complex mixture containing (in order of decreasing yield) the mixed-metal compounds  $[\text{Mo}_2\text{W}(\mu\text{-}\eta^1, \eta^5\text{-C}_5\text{H}_4)\text{Cp}_2(\text{CO})_6]$ ,  $[\text{MoW}_2(\mu\text{-}\eta^1, \eta^5\text{-C}_5\text{H}_4)\text{Cp}_2(\text{CO})_6]$  (two isomers), and  $[\text{W}_3(\mu\text{-}\eta^1, \eta^5\text{-C}_5\text{H}_4)\text{Cp}_2(\text{CO})_6]$ , along with  $[\text{WH}(\text{CO})_3\text{Cp}]$  as dominant hydrido species. The structure of the new trinuclear compounds has been determined by single crystal X-ray diffraction studies on those species with  $\text{W}_3$ ,  $\text{Mo}_2\text{W}$ , and  $\text{W}_2\text{Mo}$  metal cores. Crystals of the  $\text{W}_2\text{Mo}$  compound were found to be an equimolar mixture of both isomers detected in solution, so that two of the three metal positions are best described as 0.5 Mo + 0.5 W. Otherwise, the three crystal structures are virtually identical. These 46 electron molecules exhibit a V-shaped metal core (angle ca.  $105^\circ$ ) with a short (ca. 2.52 Å) and a long (ca. 3.12 Å) intermetallic separation, the central position being always occupied by a tungsten atom. Each of the metal atoms involved in the short bond carries out a cyclopentadienyl group and a carbonyl ligand which bridges that bond in a linear semibridging fashion. The outer metal atom has also a terminal carbonyl group. Finally, the third metal atom bears a  $\mu\text{-}\eta^1, \eta^5$ -cyclopentadienylidene ligand,  $\sigma$ -bonded to the central tungsten atom, and three terminal carbonyl groups. Variable-temperature  $^1\text{H}$  NMR spectroscopy reveals that all trinuclear compounds exhibit fluxional behavior in solution, which is thought to result from two independent rearrangements. In addition, the trimolybdenum complex undergoes a slower dynamic process which implies a proton exchange between cyclopentadienylidene and cyclopentadienyl ligands in the molecule, as suggested by 2D EXSY experiments.

## Introduction

The unsaturated complexes  $[M_2\text{Cp}_2(\text{CO})_4]$  (M = Cr, Mo, W; Cp =  $\eta^5\text{-C}_5\text{H}_5$ ) are well known to be formed through decarbonylation reactions from the corresponding hexacarbonylic precursors, this being induced by photochemical or thermal methods.<sup>1</sup> Interest in these triply bonded dimers arises mainly from their high reactivity toward many different sort of molecules,<sup>1,2</sup> but the molecular and electronic structure of these species has also attracted considerable attention.<sup>1,3</sup> In an attempt to synthesize related complexes bridged by the dppm ligand (dppm =  $\text{Ph}_2\text{PCH}_2\text{PPh}_2$ ), we studied decarbonylation reactions of the electron-precise dimers  $[M_2\text{Cp}_2(\text{CO})_4(\mu\text{-dppm})]$  (M = Mo, W). Thermal decarbonylation of the molybdenum complex promoted P–C(sp<sup>3</sup>) bond oxidative addition of the dppm ligand, yielding  $[\text{Mo}_2\text{Cp}_2(\mu\text{-CH}_2\text{PPh}_2)(\mu\text{-PPh}_2)(\text{CO})_2]$  as the major product.<sup>4</sup> Instead, both thermal and photochemical decarbonylation of the tungsten complex (1) yielded the expected triply bonded  $[\text{W}_2\text{Cp}_2(\text{CO})_2(\mu\text{-dppm})]$  (3). Surprisingly, this reaction

was found to proceed through the hydrido cyclopentadienylidene compound  $[\text{W}_2(\mu\text{-H})(\mu\text{-}\eta^1, \eta^5\text{-C}_5\text{H}_4)\text{Cp}(\text{CO})_3(\mu\text{-dppm})]$  (2), implying that a reversible and intramolecular C–H (cyclopentadienyl) oxidative addition was operating in the system (Scheme 1).<sup>5</sup>

The above observations were quite unexpected in the light of the extensive studies carried out on the decarbonylation reactions of the parent dimers  $[M_2\text{Cp}_2(\text{CO})_6]$  (4), (M = Cr, Mo, W), especially under photochemical conditions.<sup>6–13</sup> In the absence of external reagents (ligands, chlorocarbons, donor sol-

<sup>†</sup> Universidad de Oviedo.

<sup>‡</sup> Université P. et M. Curie.

<sup>⊗</sup> Abstract published in *Advance ACS Abstracts*, January 1, 1995.

(1) Winter, M. J. *Adv. Organomet. Chem.* **1989**, *29*, 101–162 and references therein.

(2) Curtis, M. D. *Polyhedron* **1987**, *6*, 759–782 and references therein.

(3) Simpson, C. Q., II; Hall, M. B. *J. Am. Chem. Soc.* **1992**, *114*, 1641–1645 and references therein.

(4) Riera, V.; Ruiz, M. A.; Villafañe, F.; Bois, C.; Jeannin, Y. *J. Organomet. Chem.* **1989**, *375*, C23–C26.

(5) Alvarez, M. A.; García, M. E.; Riera, V.; Ruiz, M. A.; Bois, C.; Jeannin, Y. *J. Am. Chem. Soc.* **1993**, *115*, 3786–3787.

(6) (a) Meyer, T. J.; Caspar, J. *Chem. Rev.* **1985**, 187–218. (b) Stufkens, D. J. In *Chemical Bonds. Better Ways to Make them and Break them*; Bernal, I., Ed.; Elsevier: Amsterdam, 1989; Chapter 3. (c) Geoffroy, G. L.; Wrighton, M. S. *Organometallic Photochemistry*; Academic Press: New York, 1979.

(7) Hughey, J. L.; Bock, C. R.; Meyer, T. J. *J. Am. Chem. Soc.* **1975**, *97*, 4440–4441.

(8) Yao, Q.; Bakac, A.; Espenson, J. H. *Organometallics* **1993**, *12*, 2010–2012.

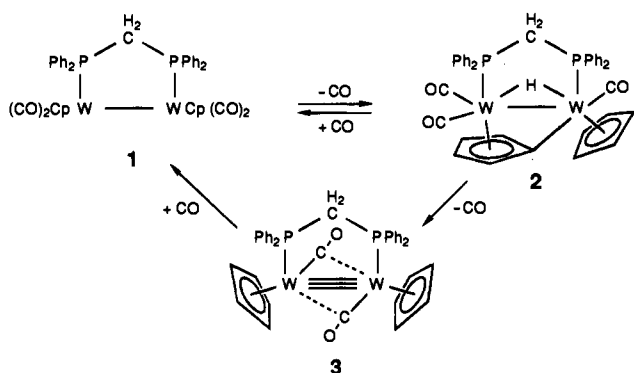
(9) Scott, S. L.; Espenson, J. H.; Zhu, Z. *J. Am. Chem. Soc.* **1993**, *115*, 1789–1797.

(10) Knorr, J. R.; Brown, T. L. *J. Am. Chem. Soc.* **1993**, *115*, 4087–4092.

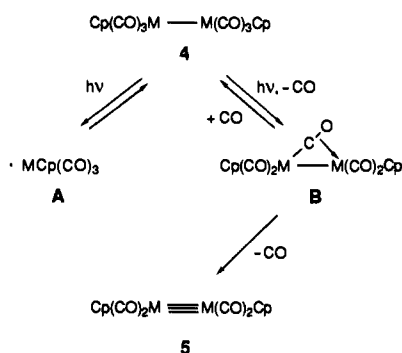
(11) (a) Hooker, R. H.; Rest, A. J. *J. Organomet. Chem.* **1983**, *254*, C25–C28. (b) Hooker, R. H.; Rest, A. J. *J. Chem. Soc., Dalton Trans.* **1990**, 1221–1229. (c) Baker, M. L.; Bloyce, P. E.; Campen, A. K.; Rest, A. J.; Bitterwolf, T. E. *Ibid.* **1990**, 2825–2832.

(12) Ginley, D. S.; Bock, C. R.; Wrighton, M. S. *Inorg. Chim. Acta* **1977**, *23*, 85–94.

Scheme 1



Scheme 2



vents, etc.), two primary products have been identified in the photolysis of complexes **4** (Scheme 2): the 17-electron tricarbonyl complex **A**, which is derived from M–M bond homolysis, and a pentacarbonylic dinuclear species **B**, formed after CO ejection from the parent dimer. This dual pathway was first recognized as early as 1975 upon flash photolysis of cyclohexane solutions of the molybdenum dimer,<sup>7</sup> and extensive complementary information (both spectroscopic and kinetic) has been obtained therefrom. It is now clear that the relative efficiencies of the pathways leading to **A** and **B** depend strongly upon reaction conditions and the nature of *M*. Thus, the pathway leading to **A** seems to prevail for the chromium system.<sup>8</sup> For molybdenum and tungsten, recent flash photolysis experiments in solution have shown that visible light favors the above pathway, whereas UV light irradiation favors the route to **B**,<sup>9,10</sup> in addition to some isomerization of the hexacarbonylic precursor.<sup>10</sup> On the other hand, intermediate **B** is the only primary photoproduct detected upon photolysis in PVC films or frozen gas matrices at low temperatures.<sup>11</sup> Contrary to the early beliefs that the final tetracarbonylic complexes **5** were formed from radicals **A**,<sup>12</sup> a series of crossover thermal experiments on the interconversion **4/5** on the molybdenum system,<sup>13</sup> and direct study of the thermal decay of photogenerated **B** at 240 K ( $M = Mo$ ) strongly suggest that it is intermediate **B**, and not **A**, which is the main precursor of the tetracarbonylic complexes **5**.<sup>10</sup>

All the above studies provide a satisfactory picture of the photochemical reactions of dimers **4**. Apparently, cyclopentadienyl C–H bond involvement has never been detected or proposed to occur in these reactions, as opposed to our findings on the dppm-bridged complex **1** (Scheme 1). However, if such a process could be reversible, as found for complex **2**, it could have passed easily undetected in the reactions of the nonbridged dimers **4**. The latter possibility, added to the relevance of C–H

activation processes,<sup>14</sup> prompted us to examine again the photochemical decarbonylation reactions of the dimers **4** under similar conditions to those employed in the dppm-bridged complex **1**, that is, toluene solutions at low temperatures. The results of this study, here reported, show that the novel trinuclear cyclopentadienylidene complexes  $[M_3(\mu-\eta^1, \eta^5-C_5H_4)Cp_2(CO)_6]$  ( $M = Mo, W$ ) are formed under these conditions. The latter have been isolated as crystalline solids and have been fully characterized both in solution and in the solid state, while related mixed-metal complexes having  $Mo_2W$  or  $MoW_2$  metal skeletons have been also obtained by a modification of the experimental procedure. The synthesis of the tritungsten complex was reported in our early communication,<sup>5</sup> although full structural elucidation was not possible at that time. Overall, these results prove that C–H activation processes do occur during photolysis of dimers **4** when *M* is Mo or W. However, no evidence for this phenomenon has been obtained in the chromium system. Although cyclopentadienyl C–H cleavages are well-documented processes, almost all examples involve bis-cyclopentadienyl complexes of the early transition metals,<sup>15,16</sup> while there is to our knowledge only one previous example of related bond cleavages in photochemical reactions of transition metal carbonyl dimers having cyclopentadienyl ligands.<sup>17</sup>

## Results and Discussion

**Photochemical Synthesis of Trinuclear Complexes.** Photolysis of toluene solutions of  $[W_2Cp_2(CO)_6]$  at  $-35^\circ C$  under a gentle nitrogen purge yields a mixture containing the known complex  $[W_2(\mu-H)_2Cp_2(CO)_4]$ <sup>18</sup> and the new trinuclear compound  $[W_3(\mu-\eta^1, \eta^5-C_5H_4)Cp_2(CO)_6]$  (**6**) as major species. Minor amounts of  $[W_2Cp_2(CO)_4]$  and  $[WH(CO)_3Cp]$  are also

(14) (a) Collman, J. P.; Hegedus, L. S.; Norton, J. R.; Finke, R. G. *Principles and Applications of Organotransition Metal Chemistry*; University Science Books: Mill Valley, CA, 1987; pp 295–305. (b) Crabtree, R. H. *Angew. Chem., Int. Ed. Engl.* **1993**, *32*, 789–805. (c) Ryabov, A. D. *Chem. Rev.* **1990**, *90*, 403–424. (d) Jones, W. D.; Feher, F. J. *Acc. Chem. Res.* **1989**, *22*, 91–100. (e) Crabtree, R. H. *Chem. Rev.* **1985**, *85*, 245–269. (f) Brookhart, M.; Green, M. L. H. *J. Organomet. Chem.* **1983**, *250*, 395–408.

(15) Reviews: (a) Coville, N. J.; du Plooy, K. E.; Pickl, W. *Coord. Chem. Rev.* **1992**, *116*, 1–267. (b) Pez, G. P.; Armor, J. N. *Adv. Organomet. Chem.* **1981**, *19*, 1–50.

(16) (a) Ho, J.; Rousseau, R.; Stephan, D. W. *Organometallics* **1994**, *13*, 1918–1926. (b) Berry, D. H.; Koloski, T. S.; Carroll, P. J. *Organometallics* **1990**, *9*, 2952–2962. (c) Casey, C. P. *J. Organomet. Chem.* **1990**, *400*, 205–221. (d) Grebenik, P. D.; Green, M. L. H.; Kelland, M. A.; Leach, J. B.; Mountford, P. *J. Chem. Soc., Chem. Commun.* **1989**, 1397–1399. (e) Kool, L. B.; Rausch, M. D.; Alt, H. G.; Herberhold, M.; Thewalt, U.; Honold, B. *J. Organomet. Chem.* **1986**, *310*, 27–34. (f) Albinati, A.; Togni, A.; Venanzi, L. M. *Organometallics* **1986**, *5*, 1785–1791. (g) Howarth, O. W.; McAteer, C. H.; Moore, P.; Morris, G. E.; Alcock, N. W. *J. Chem. Soc., Dalton Trans.* **1982**, 541–548. (h) Barral, M. C.; Green, M. L. H.; Jimenez, R. *Ibid.* **1982**, 2495–2498. (i) Bashkin, J.; Green, M. L. H.; Poveda, M. L.; Prout, K. *Ibid.* **1982**, 2485–2494. (j) Gell, K. I.; Harris, T. V.; Schwartz, J. *Inorg. Chem.* **1981**, *20*, 481–488. (k) Pasynskii, A. A.; Skripkin, Y. V.; Kalinnikov, V. T.; Porai-Koshits, M. A.; Antsyshkina, A. S.; Sadikov, G. G.; Ostrikova, V. N. *J. Organomet. Chem.* **1980**, *201*, 269–281. (l) Lemenovskii, D. A.; Fedin, V. P.; Aleksandrov, A. V.; Slovohtov, Y. L.; Struchkov, Y. T. *Ibid.* **1980**, *201*, 257–268. (m) Berry, M.; Cooper, J.; Green, M. L. H.; Simpson, S. J. *J. Chem. Soc., Dalton Trans.* **1980**, 29–40. (n) Berry, M.; Elmitt, K.; Green, M. L. H. *Ibid.* **1979**, 1950–1958. (o) Hoxmeier, R. J.; Blicksenderfer, J. R.; Kaesz, K. D. *Inorg. Chem.* **1979**, *18*, 3453–3461. (p) Berry, M.; Davies, S. G.; Green, M. L. H. *J. Chem. Soc., Chem. Commun.* **1978**, 99–100. (q) Guggenberger, L. *J. Inorg. Chem.* **1973**, *12*, 294–301.

(17) The photochemical reaction of  $[Ru_2(\eta^5-C_5H_5)_2(CO)_4]$  has been shown to yield the cyclopentadienylidene complexes  $[Ru_2(CO)_4(\eta^5-C_5H_5)(\mu-\eta^1, \eta^5-C_5H_4)Ru(CO)_2(\eta^5-C_5H_5)]$ , and  $[Ru_4(\mu_3-\eta^1, \eta^1, \eta^5-C_5H_4)_2(\eta^5-C_5H_5)_2(CO)_6]$ . See: Feasey, N. D.; Forrow, N. J.; Hogarth, G.; Knox, S. A. R.; Macpherson, K. A.; Morris, M. J.; Orpen, A. G. *J. Organomet. Chem.* **1984**, *267*, C41–C44.

(18) (a) Alt, H. G.; Mahmoud, K. A.; Rest, A. J. *Angew. Chem., Int. Ed. Engl.* **1983**, *22*, 544–545. (b) Mahmoud, K. A.; Rest, A. J.; Alt, H. G. *J. Chem. Soc., Dalton Trans.* **1984**, 182–197.

(13) Turaki, N. N.; Huggins, J. M. *Organometallics* **1985**, *4*, 1766–1769.

detected in the reaction mixture. However, both IR and NMR monitoring of the reaction reveal that the mononuclear hydride is the main hydrido species formed at the beginning of the reaction, which then steadily decays to yield the dinuclear dihydride, in agreement with previous photochemical studies on that hydrido complex.<sup>18</sup> Finally, in order to exclude possible sources of hydrido ligands, the photolytic reaction was performed in deuterated toluene. <sup>1</sup>H NMR analysis of the resulting mixture revealed a composition similar to that one resulting from the reactions in the nondeuterated solvent. Therefore, the solvent can be safely excluded as the origin of the hydrido ligands present in the products.

Under similar conditions to those used in the synthesis of **6**, the complex  $[\text{Mo}_2\text{Cp}_2(\text{CO})_6]$  affords a mixture containing  $[\text{MoH}(\text{CO})_3\text{Cp}]$ ,  $[\text{Mo}_2\text{Cp}_2(\text{CO})_4]$ , and the new complex  $[\text{Mo}_3(\mu-\eta^1, \eta^5\text{-C}_5\text{H}_4)\text{Cp}_2(\text{CO})_6]$  (**7**) as major species. The relative amount of mononuclear hydride isolated was found to be strongly dependent on experimental conditions. For example, prolonged reaction times consumed it almost completely, again in agreement with previous studies, which have shown its transformation into the tetracarbonyl dimer under photochemical conditions.<sup>18</sup> On the other hand, the trimolybdenum species **7** was found to be thermally unstable. Thus, toluene solutions of **7** decomposed to yield  $[\text{Mo}_2\text{Cp}_2(\text{CO})_4]$  (as major carbonyl-containing product) within a few minutes at room temperature. The same, but at lower rate, was observed in the solid state. At  $-30^\circ\text{C}$ , however, the solutions of complex **7** can be safely handled during several hours.

In order to test an hypothesis that would explain the formation of the trinuclear complexes **6** and **7** (see later), equimolar amounts of  $[\text{W}_2\text{Cp}_2(\text{CO})_6]$  and  $[\text{Mo}_2\text{Cp}_2(\text{CO})_4]$  were photolyzed in toluene at  $-35^\circ\text{C}$  under a nitrogen purge. This afforded a quite complex mixture whose exact composition was found to depend on reaction time, concentration, or even the rate of flow of the purge. In addition to variable amounts of unreacted  $[\text{Mo}_2\text{Cp}_2(\text{CO})_4]$ , the main hydrido species formed was  $[\text{WH}(\text{CO})_3\text{Cp}]$ , and trace amounts of  $[\text{MoH}(\text{CO})_3\text{Cp}]$  were also isolated. This follows from direct IR and NMR monitoring of the reaction mixture as well as chromatographic workup. Finally, a mixture of the trinuclear complexes **6**, **7**,  $[\text{Mo}_2\text{W}(\mu-\eta^1, \eta^5\text{-C}_5\text{H}_4)\text{Cp}_2(\text{CO})_6]$  (**8**), and two isomers with the formula  $[\text{MoW}_2(\mu-\eta^1, \eta^5\text{-C}_5\text{H}_4)\text{Cp}_2(\text{CO})_6]$  (**9**, **10**) were also formed. These trinuclear complexes can be reasonably separated by column chromatography (except for **9** and **10**) and finally isolated by recrystallization as pure, air-sensitive solids. New species are rapidly formed upon brief exposure to air of all these trinuclear compounds. They probably retain the trimetallic skeleton, as suggested by <sup>1</sup>H NMR data, but unfortunately purification and full structural characterization of these products has not been possible. On the other hand, compounds **9** (W–W≡Mo skeleton) and **10** (Mo–W≡W skeleton) could not be separated from each other by either method, even when they do not seem to interconvert spontaneously. In fact, they were found to co-crystallize (see later). As for other products in the reaction mixture, the exact relative amounts of the trinuclear compounds would depend upon experimental conditions. Typically, the dimolybdenum–tungsten complex **8** was the major species, followed by the ditungsten–molybdenum isomers **9** and **10** (produced in similar relative amounts) and only very minor amounts of **6** and **7**. No experimental conditions for the selective formation of any of the mixed-metal species **8**, **9**, or **10** could be found.

**Crystal Structures of the Trinuclear Complexes.** Single crystals suitable for X-ray diffraction studies could be obtained for compounds **6** and **8**. The isomers **9** and **10** co-crystallized,

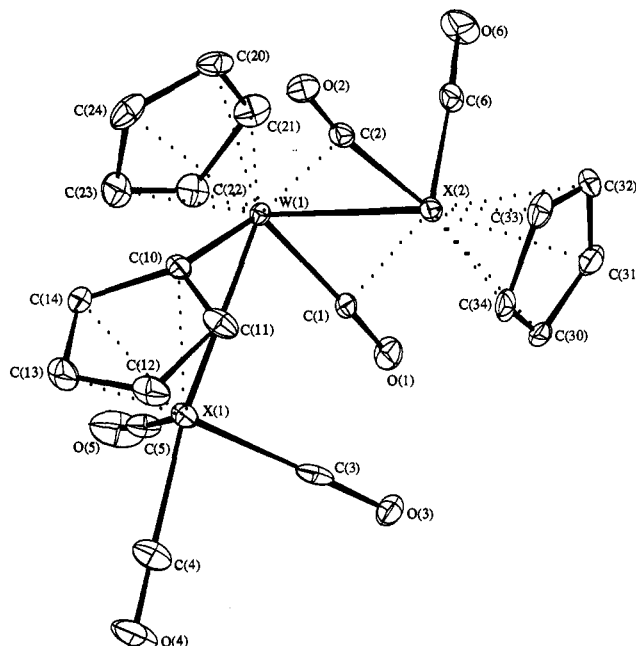


**Figure 1.** CAMERON diagram of the molecular structure of  $[\text{MoW}_2(\mu-\eta^1, \eta^5\text{-C}_5\text{H}_4)\text{Cp}_2(\text{CO})_6]$ . X(1) and X(2) are  $0.5\text{Mo} + 0.5\text{W}$ , which corresponds to an equimolar mixture of compounds **9** and **10** (see text). Ellipsoids represent 20% of probability. Identical diagrams were obtained for compounds **6** [X(1) = X(2) = W] and **8** [X(1) = X(2) = Mo].

yielding single crystals shown to contain a disorder in two of the three metal positions, each with a composition 50% Mo and 50% W (because of this, we will refer to this sort of crystals as **9:10**). Apart from the latter, the three structures are virtually identical (Figure 1), not only concerning unit cell parameters (Table 1) but also bond distances and angles (Table 2), which is not too surprising given the similar sizes of the molybdenum and tungsten atoms. The molecules exhibit a V-shaped trimetal core, with an intermetallic angle of *ca.*  $105^\circ$  and two very different intermetallic distances (*ca.* 3.12 and 2.52 Å). These values can be identified respectively with formal metal–metal bonds of orders one and three, by comparison with representative examples,<sup>19</sup> and consideration of the 18-electron rule for the molecule. One of the remarkable features in the structure is the presence of a cyclopentadienylidene ligand bridging the long metal–metal vector in a  $\eta^1, \eta^5$  fashion, with the C(10) atom  $\sigma$ -bonded to the central metal atom, which is tungsten in all cases. Overall, the structure can be described as derived from the triply bonded complexes  $[\text{M}_2(\text{CO})_4\text{L}_2]$  (M = Cr, Mo, W;  $\text{L}_2 = \text{Cp}$  or related  $\eta^5$ -ligands)<sup>1</sup> after replacement of a carbonyl ligand by the two-electron fragment  $\text{M}(\text{CO})_3(\text{C}_5\text{H}_4)$ . As a result of the steric requirements of the latter, only two carbonyl ligands (C(1)–O(1) and C(2)–O(2)) bridge the triple bond, whereas the third carbonyl group (C(6)–O(6)) is coordinated in a terminal way. This yields a distorted tetrahedral environment around each metal center involved in the triple bond, if we consider the Cp ligands and the  $\text{M}(\text{CO})_3(\text{C}_5\text{H}_4)$  moiety as occupying a single coordination position. We note that this

(19) Single bond lengths: (a) 3.222(1) Å for  $[\text{W}_2(\text{CO})_6\text{Cp}_2]$ ; See: Adams, R. D.; Collins, D. M.; Cotton, F. A. *Inorg. Chem.* **1974**, *13*, 1086–1090. (b) 3.179(2) Å for  $[\text{W}_2(\mu\text{-H})(\mu-\eta^1, \eta^5\text{-C}_5\text{H}_4)\text{Cp}(\text{CO})_2(\text{CN}^i\text{Bu})(\mu\text{-dppm})]$ ; see ref 5. Triple bond lengths: (c) 2.503(1) Å for  $[\text{W}_2(\text{CO})_4\text{L}_2]$  (L = CpCo{P(O)(OEt)}<sub>2</sub>); see: Klaul, W.; Muller, A.; Herbst, R.; Egert, E. *Organometallics* **1987**, *6*, 1824–1826. (d) 2.515(1) Å for  $[\text{W}_2(\text{CO})_2(\mu\text{-dppm})\text{Cp}_2]$ ; see ref 5. (e) 2.586(1) Å for  $[\text{W}_2(\mu\text{-CO})_2(\text{CO})(\eta\text{-PhC}_2\text{Ph})\{\eta^5\text{-C}_5\text{Ph}_4(\text{C}_6\text{H}_4\text{Me-4})\}]$ ; see: Carriedo, G. A.; Howard, J. A. K.; Lewis, D. B.; Lewis, G. E.; Stone, F. G. A. *J. Chem. Soc., Dalton Trans.* **1985**, 905–912.

Table 1. Experimental Data for the X-ray Diffraction Studies

	6	8	9:10
mol formula	$C_{21}H_{14}O_6W_3$	$C_{21}H_{14}Mo_2O_6W$	$C_{21}H_{14}MoO_6W_2$
mol wt	912.9	738.07	825.98
cryst syst	orthorhombic	orthorhombic	orthorhombic
space group	<i>Pcab</i>	<i>Pcab</i>	<i>Pcab</i>
<i>a</i> , Å	15.738(3)	15.733(2)	15.729(3)
<i>b</i> , Å	15.725(8)	15.760(3)	15.742(5)
<i>c</i> , Å	16.503(3)	16.530(2)	16.521(2)
<i>V</i> , Å <sup>3</sup>	4084(4)	4098(2)	4091(3)
<i>Z</i>	8	8	8
<i>D</i> <sub>calcd</sub> , g cm <sup>-3</sup>	2.97	2.39	2.68
<i>F</i> (000)	3280	2768	3024
$\mu$ , cm <sup>-1</sup>	172.6	69.35	120.9
temp, °C	18	18	18
cryst size, mm	0.45 × 0.25 × 0.15	0.65 × 0.45 × 0.20	0.65 × 0.45 × 0.20
diffractometer	nonius CAD4	nonius CAD4	CAD4F
radiation	Mo K $\alpha$	Mo K $\alpha$	Mo K $\alpha$
monochromator	graphite	graphite	graphite
scan type	$\omega - 2\theta$	$\omega - 2\theta$	$\omega - 2\theta$
scan width	0.8 + 0.34 tan $\theta$	0.8 + 0.34 tan $\theta$	0.8 + 0.34 tan $\theta$
$\theta$ range, deg	1–25	1–25	1.5–25
standard rflns	2	2	2
no. of measd rflns	3583	3602	3592
no. of rflns used, $I \geq 3\sigma(I)$	2004	2596	2680
no. of refined parameters	274	274	273
<i>R</i>	0.041	0.034	0.033
<i>R</i> <sub>w</sub>	0.046	0.037	0.040

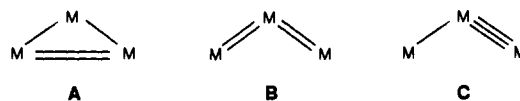
Table 2. Selected Bond Distances (Å) and Angles (deg) in the Trinuclear Compounds 6, 8, and 9:10

	6 <sup>a</sup>	8 <sup>b</sup>	9:10 <sup>c</sup>
W(1)–X(1)	3.119(1)	3.1320(9)	3.127(1)
W(1)–X(2)	2.527(1)	2.5230(9)	2.526(1)
W(1)–C(1)	1.94(2)	1.98(1)	1.96(1)
X(2)–C(1)	2.42(2)	2.46(1)	2.47(1)
X(2)–C(2)	1.93(2)	1.92(1)	1.97(1)
W(1)–C(2)	2.50(2)	2.46(1)	2.51(1)
X(2)–C(6)	1.97(2)	1.96(1)	1.96(1)
X(1)–C(3)	1.91(3)	1.95(1)	1.98(2)
X(1)–C(4)	1.99(3)	1.98(1)	2.00(1)
X(1)–C(5)	1.97(3)	1.97(1)	1.99(2)
W(1)–C(10)	2.13(2)	2.11(1)	2.08(1)
X(1)–C(10)	2.25(2)	2.21(1)	2.21(1)
X(1)–C(11)	2.29(2)	2.28(1)	2.28(1)
X(1)–C(14)	2.33(2)	2.30(1)	2.30(1)
X(1)–C(12)	2.35(2)	2.38(1)	2.35(2)
X(1)–C(13)	2.35(2)	2.37(1)	2.37(1)
W(1)–Cp <sup>1</sup> <sup>d</sup>	2.34(2)	2.35(1)	2.35(1)
X(2)–Cp <sup>2</sup> <sup>e</sup>	2.36(2)	2.35(1)	2.36(1)
X(1)–W(1)–X(2)	105.2(3)	104.34(3)	104.76(3)
C(1)–W(1)–X(2)	64.0(6)	65.1(3)	65.3(4)
C(2)–X(2)–W(1)	66.7(6)	65.6(3)	66.5(4)
C(6)–X(2)–W(1)	86.6(6)	87.0(3)	88.2(4)
O(1)–C(1)–W(1)	164.4(17)	165.6(10)	165.9(11)
O(2)–C(2)–X(2)	170.7(18)	167.0(9)	168.8(12)
O(6)–C(6)–X(2)	172.3(17)	176.6(11)	174.5(14)
O(5)–C(5)–X(1)	179.1(21)	177.2(14)	176.6(17)
O(4)–C(4)–X(1)	177.0(25)	176.7(12)	178.9(16)
O(3)–C(3)–X(1)	179.1(19)	177.1(11)	177.1(15)

<sup>a</sup> X(1) and X(2) are W atoms. <sup>b</sup> X(1) and X(2) are Mo atoms. <sup>c</sup> X(1) and X(2) are 0.5Mo + 0.5W (see text and Figure 1). <sup>d</sup> Averaged metal to C(20)/C(24) length. <sup>e</sup> Averaged metal to C(30)/C(34) length.

effect is also observed in the structure of  $[W_2(\mu-CO)_2(CO)(\eta^2-PhC_2Ph)Cp\{\eta^5-C_5Ph_4(C_6H_4Me-4)\}]$ ,<sup>19e</sup> which is related to those of our trinuclear complexes by replacing the two-electron alkynyl ligand by the cyclopentadienylidene  $M(CO)_3(C_5H_4)$  moiety. The alkyne group in the previous ditungsten complex binds the metal atom so that the C–C vector is almost normal to the metal–metal vector.<sup>19e</sup> Interestingly, the same can be said of the X(1)–C(10) vector relative to the triple bond direction in our trinuclear compounds.

Chart 1



The carbonyl ligands across the triple metal–metal bond in compounds 6 to 10 ( $M-C$  and  $M-C$  lengths *ca.* 1.92–1.98 Å and 2.42–2.51 Å, respectively;  $M-C-O$  and  $C-M\equiv M$  angles *ca.* 165–170° and 64–67°, respectively) belong to the type II linear semibridging class,<sup>20</sup> as usually found for the above-mentioned unsaturated dimers  $[M_2(CO)_4L_2]$ .<sup>1</sup>

The geometrical parameters involving the cyclopentadienylidene ligand in compounds 6 to 10 indicate an almost undistorted  $\eta^5$ -coordination to the metal–tricarbonyl fragment. Although we are not aware of any previous crystallographic study involving cyclopentadienylidene ligands  $\sigma$ -bonded to tungsten atoms, the C(10)–W(1) distances in our trinuclear compounds (*ca.* 2.10 Å) have about the expected value for a  $W-C(sp^2)$  single bond. This gives further support to a  $\eta^1, \eta^5$  description for the coordination of the cyclopentadienyl ligand in the trinuclear compounds. We also note that similar distances were found in two independent studies on the dimolybdenum complex  $[Mo_2(\mu-\eta^1, \eta^5-C_5H_4)Cp_2(CO)_3]$  (*ca.* 2.1 Å).<sup>16i,21</sup>

Compounds 6 to 10 are 46 valence electron trimetal species. According to the 18-electron rule, this requires the presence of four metal–metal bonds. In a topological sense, the latter can be achieved in three different ways (A to C in Chart 1). The triangular structure A is the most common one, possibly because it contains the maximum number of  $\sigma$ -type metal–metal interactions. By contrast, we are only aware of one example of structure B.<sup>22</sup> Finally, the metal skeleton exhibited by compounds 6 to 10 (structure C) is also quite unusual, as only two other examples  $[MoW_2\{\mu-\sigma, \sigma': \eta^4-C(Ph)C(Ph)C(C_6H_4Me-4)C(C_6H_4Me-4)\}(CO)_6Cp_2]$ <sup>23</sup> and  $[FeMo_2Cp_2\{\mu-RPC_6H_4PR\}-$

(20) Crabtree, R. H.; Lavin, M. *Inorg. Chem.* **1986**, *25*, 805–812.

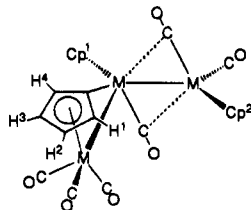
(21) Herrmann, W. A.; Kriechbaum, G.; Bauer, C.; Guggolz, E.; Ziegler, M. L. *Angew. Chem., Int. Ed. Engl.* **1981**, *20*, 815–817.

(22) Davidson, J. L.; Davidson, K.; Lindsell, E.; Murrall, N. W.; Welch, A. J. *J. Chem. Soc., Dalton Trans.* **1986**, 1677–1688.

Table 3. IR Data for New Compounds<sup>a</sup>

compd	$\nu(\text{CO})/\text{cm}^{-1}$
[W <sub>3</sub> ( $\mu$ - $\eta^1$ , $\eta^5$ -C <sub>5</sub> H <sub>4</sub> )Cp <sub>2</sub> (CO) <sub>6</sub> ] (6)	1977 (vs), 1925 (s), 1909 (m, sh), 1875 (s), 1833 (m)
[Mo <sub>3</sub> ( $\mu$ - $\eta^1$ , $\eta^5$ -C <sub>5</sub> H <sub>4</sub> )Cp <sub>2</sub> (CO) <sub>6</sub> ] (7)	1986 (vs), 1929 (vs), 1888 (vs), 1843 (m)
[Mo <sub>2</sub> W( $\mu$ - $\eta^1$ , $\eta^5$ -C <sub>5</sub> H <sub>4</sub> )Cp <sub>2</sub> (CO) <sub>6</sub> ] (8)	1982 (vs), 1928 (vs), 1885 (s), 1833 (m)
[MoW <sub>2</sub> ( $\mu$ - $\eta^1$ , $\eta^5$ -C <sub>5</sub> H <sub>4</sub> )Cp <sub>2</sub> (CO) <sub>6</sub> ] (9, 10) <sup>b</sup>	1980 (vs), 1927 (s), 1881 (s), 1832 (m)

<sup>a</sup> In toluene solution. <sup>b</sup> Relative molar ratio *ca.* 1:1 (see text).

Table 4. <sup>1</sup>H NMR Data for New Compounds<sup>a</sup>

compd	$\delta/\text{ppm}^b$					
	H <sup>1</sup>	H <sup>2</sup>	H <sup>3</sup>	H <sup>4</sup>	Cp <sup>1</sup>	Cp <sup>2</sup>
6 <sup>c,d</sup>	5.54 (dt)	4.60 (td)	4.51 (td)	3.87 (dt)	4.74	4.68
7 <sup>e</sup>	5.71 (br)	4.42 (br)	4.23 (br)	3.59 (br)	4.59	4.52
8 <sup>f</sup>	5.59 (br)	4.69 (br)	4.59 (br)	3.83 (br)	4.84	4.80
9 <sup>c,g</sup>	5.65 (dt)	4.65 (td)	4.52 (td)	3.86 (br)	4.75	4.74
10 <sup>c,g</sup>	5.46 (dt)	4.62 (br)	4.54 (br)	3.79 (br)	4.79	4.72

<sup>a</sup> Measured at 400.13 MHz in toluene-*d*<sub>8</sub> solutions, except for compounds 9 and 10 (measured at 300.13 MHz). <sup>b</sup> Labeling according to the figure shown below. <sup>c</sup>  $J(\text{H}^1\text{H}^2) = J(\text{H}^2\text{H}^3) = J(\text{H}^3\text{H}^4) = 2.6$  Hz;  $J(\text{H}^1\text{H}^3) = J(\text{H}^1\text{H}^4) = J(\text{H}^2\text{H}^4) = 1.3$  Hz. <sup>d</sup> At 230 K. <sup>e</sup> At 193 K. <sup>f</sup> At 293 K. <sup>g</sup> At 258 K.

Table 5. <sup>13</sup>C{<sup>1</sup>H} NMR Data for New Compounds<sup>a</sup>

atom type <sup>b</sup>	$\delta/\text{ppm}$		
	compd 6 <sup>c</sup>	compd 7 <sup>d</sup>	compd 8 <sup>e</sup>
CO	238.1, 226.4, 223.8	244.7, 240.9, 240.5	246.2, 235.3, 232.2
	223.1, 220.1, 215.4	233.5, 231.0, 226.2	231.7, 229.5, 225.5
$\mu$ -C	183.2	208.5	193.5
C <sup>1,4</sup> <sup>f</sup>	108.7, 106.5	109.9, 107.3	111.2, 107.4
C <sup>2,3</sup> <sup>f</sup>	84.8, 84.5	84.9, 84.1	86.6, 85.8
Cp <sup>1,2</sup> <sup>f</sup>	97.1, 91.4	96.9, 91.9	96.2, 92.1

<sup>a</sup> Measured at 75.47 MHz in CD<sub>2</sub>Cl<sub>2</sub> solutions. <sup>b</sup> Labeling according to the structure in Table 4. <sup>c</sup> At 230 K. <sup>d</sup> At 193 K. <sup>e</sup> At 213 K. <sup>f</sup> No individual assignment implied.

(CO)<sub>5</sub> (R = Ph)<sup>24</sup> appear to have been characterized structurally. Interesting, the latter complex adopts a triangular structure (A) when R = <sup>t</sup>Bu, which suggests that the energy difference between structures A and C must be modest. Therefore, the reasons why complexes 6 and 10 adopt the open structure C rather than the triangular A may be of a rather subtle nature. In fact, the hypothesis that a structure of the latter type would not be much higher in energy will be of help when analyzing the dynamics of these trinuclear complexes in solution, as we will discuss next.

**Solution Structure and Dynamics.** The relevant spectroscopic data in solution for complexes 6 to 10 are collected in Tables 3 (IR), 4 (<sup>1</sup>H NMR), and 5 (<sup>13</sup>C{<sup>1</sup>H} NMR). They all show similar characteristics, indicating that these trinuclear complexes are also isostructural in solution. Furthermore, the low-temperature NMR spectra and the  $\nu(\text{CO})$  pattern are fully consistent with the structures found in the solid state. The lack of chemical equivalence of all six CO ligands, the four C–H

(cyclopentadienylidene ligand) groups and both Cp ligands is readily apparent in the <sup>13</sup>C and <sup>1</sup>H NMR spectra of compounds 6 to 10. The cyclopentadienylidene atoms  $\sigma$ -bonded to the central tungsten atom (C(10) in Figure 1) give rise to a <sup>13</sup>C resonance in the range 183.2–208.5 ppm. These values are among the highest reported for transition metal cyclopentadienylidene complexes (*ca.* 190 ppm for the complexes [Ru(CO)L( $\mu$ - $\eta^1$ , $\eta^5$ -C<sub>5</sub>H<sub>4</sub>)ZrCp<sub>2</sub>(CO)] with L = CO, PMe<sub>3</sub>).<sup>25</sup> It would be tempting to identify this high deshielding with some  $\pi$  bonding or "carbenoid" contribution<sup>16,21</sup> to the W(1)–C(10) bond, but we note that there is no indication for this contribution in the solid-state structure of our compounds.

Full assignment of the <sup>1</sup>H NMR spectrum (Table 4) of the trinuclear compounds has been carried out in detail for compound 6, and it is assumed to be valid also for complexes 7 to 10. The assignment is based on the identification of a single resonance. Once this is done, the rest follows from standard selective decoupling experiments or NOE information obtained from EXSY spectra (see below). To start with, it was clear that the H atoms closer to the bridgehead carbon atom of the C<sub>5</sub>H<sub>4</sub> ligand (H<sup>1</sup>/H<sup>4</sup>) were responsible for the resonances at 5.54 and 3.87 ppm, but we could not clearly distinguish one from the other on the basis of the chemical shifts or coupling constants. However, examination of the solid-state structures of compounds 6 to 10 reveals that H<sup>4</sup> is relatively close to the hydrogen atoms of the Cp<sup>1</sup> ligand (minimum separation estimated to be *ca.* 1.9 Å, after allowing free rotation of the cyclopentadienyl group), whereas H<sup>1</sup> is more distant from the hydrogen atoms of Cp<sup>2</sup> (minimum separation estimated analogously to be *ca.* 2.5 Å). Therefore, as other hydrogen atoms are almost equally separated from H<sup>1</sup> or H<sup>4</sup>, we would expect a faster longitudinal relaxation (shorter T<sub>1</sub>) for H<sup>4</sup>, as a result of more efficient H–H dipolar relaxation, which is well known to be strongly dependent on internuclear distances.<sup>26</sup>

T<sub>1</sub> measurements on compound 6 at 230 K yielded the values T<sub>1</sub> = 0.8 s ( $\delta$  = 3.87 ppm) and 2.4 s ( $\delta$  = 5.54 ppm). These figures have some contribution from mutual chemical exchange (see later), so the intrinsic difference in relaxation rates is possibly somewhat higher. In any case, these values clearly indicate that the 3.87 ppm resonance is due to H<sup>4</sup>. As we have said, once this is established, the identification of all other cyclopentadienylidene resonances is straightforward. As for the Cp ligands, two independent methods lead to the same assignment. In first place, and following the previous reasoning, Cp<sup>1</sup> can be identified because it is expected to cause a significant NOE enhancement on the H<sup>4</sup> resonance. This is the case for the Cp resonance at  $\delta$  = 4.74 ppm, as inspection of the positive cross-peaks in the EXSY spectrum of 6 reveals (see later; Figure 2). Alternatively, Cp<sup>1</sup> can be identified because it is expected to experience a longitudinal relaxation faster than Cp<sup>2</sup>. This follows in part from the close proximity between Cp<sup>1</sup> and H<sup>4</sup>. In addition, the latter probably restricts somewhat the rotation of the Cp<sup>1</sup> ligand, which then is to be slower than that of Cp<sup>2</sup>. This would lead to a longer local correlation time ( $\tau_c$ ) for Cp<sup>1</sup>

(23) Carriedo, G. A.; Howard, J. A. K.; Jeffery, J. C.; Sneller, K.; Stone, F. G. A.; Weerasuria, A. M. M. *J. Chem. Soc., Dalton Trans.* **1990**, 953–958.

(24) Kyba, E. P.; Kerby, M. C.; Kashyap, R. P.; Hassett, K. L.; Davis, R. E. *J. Organomet. Chem.* **1988**, 346, C19–C23.

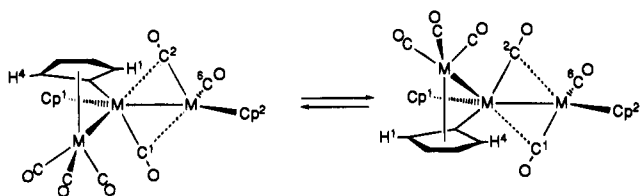
(25) Casey, C. P.; Palermo, R. E.; Jordan, R. F.; Rheingold, A. L. *J. Am. Chem. Soc.* **1985**, 107, 4597–4599.

(26) Sanders, J. K. M.; Hunter, B. K. *Modern NMR Spectroscopy*; 2nd ed.; Oxford University Press: Oxford, U.K., 1993.

**Table 6.** Coalescence Data for the  $^1H$  NMR Spectra of Complexes 6 to 10<sup>a</sup>

compd	Cp <sup>1</sup> /Cp <sup>2</sup> exchange			H <sup>2</sup> /H <sup>3</sup> exchange		
	$T_c/K$	$\Delta\nu/Hz$	$\Delta G^\ddagger/kJ mol^{-1}$	$T_c/K$	$\Delta\nu/Hz$	$\Delta G^\ddagger/kJ mol^{-1}$
6	297 ± 1	28 ± 1	62.5 ± 0.3	297 ± 1	40 ± 1	61.6 ± 0.3
7	225 ± 1	19 ± 1	47.5 ± 0.3	233 ± 2	57 ± 1	47.2 ± 0.5
8		not observed		295 ± 2	20 ± 1	62.9 ± 0.5
9		not observed			not measured	
10	290 ± 2	22 ± 1	61.6 ± 0.5	290 ± 2	22 ± 1	61.6 ± 0.5

<sup>a</sup> Measured in toluene solutions at 300.13 MHz, except for compound 6 (400.13 MHz) and 8 (200.13 MHz). Chemical shift differences ( $\Delta\nu$ ) changed with temperature; the values quoted are those corresponding to temperatures *ca.* 20 K below coalescence.

**Scheme 3.** Representation of the Rearrangement Proposed to Occur for Compounds 6 to 10 in Solution

and, therefore, also to a more efficient relaxation (shorter  $T_1$ ).<sup>26</sup> In fact,  $T_1$  for the 4.74 ppm resonance at 230 K is found to be 1.4 s while the other cyclopentadienyl ligand ( $\delta = 4.68$  ppm) relaxes much more slowly ( $T_1 = 6.6$  s).

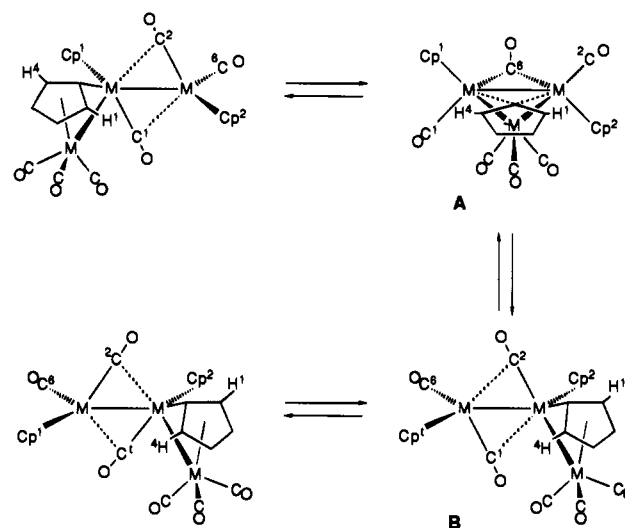
As we have stated, the NMR data just discussed, which are fully consistent with the solid-state structures of compounds 6 to 10, were obtained at low temperatures in general. As the temperature is increased, the following modifications are observed in the  $^1H$  spectra of the trimetallic complexes:

- The resonances due to H<sup>2</sup> and H<sup>3</sup> coalesce into a single one in all cases.
- The resonances due to H<sup>1</sup> and H<sup>4</sup> broaden and eventually disappear from the spectra in all cases.
- The resonances due to Cp<sup>1</sup> and Cp<sup>2</sup> coalesce into a single one *only* for compounds 6, 7, and 10, that is, for compounds exhibiting a *homometallic* triple bond.

We have been able to measure most (but not all) of the corresponding coalescence temperatures. From these values we have obtained an estimation<sup>27</sup> of the free energy of activation for the processes involved (Table 6). Except for the trimolybdenum complex 7, the values for all other complexes are almost the same (*ca.* 62 kJ mol<sup>-1</sup>). Furthermore, when both H<sup>2</sup>/H<sup>3</sup> and Cp<sup>1</sup>/Cp<sup>2</sup> coalescences are observed in the same compound (6, 7, 10), the corresponding activation energies are virtually identical within experimental error.

Although it is quite reasonable to assume that the dynamic process equalizing the magnetic environments of H<sup>2</sup> and H<sup>3</sup> should cause the same effect on H<sup>1</sup> and H<sup>4</sup>, direct observation of this effect was not possible. Even for the complex with higher thermal stability (6) the averaged resonance for H<sup>1</sup>/H<sup>4</sup> was not yet hinted at 90 °C. This is most likely due to their large chemical shift difference. However, in order to obtain direct evidence for this exchange, we carried out 2D EXSY experiments for our trinuclear compounds. They were performed in the phase-sensitive mode in order to detect both exchange and cross-relaxation (NOE) phenomena. In this experiment, cross peaks due to chemical exchange appear with the same phase as diagonal peaks, whereas those due to cross

(27) Calculated using the modified Eyring equation:  $\Delta G^\ddagger = 19.14T_c[9.97 + \log(T_c/\Delta\nu)]$  (J mol<sup>-1</sup>). The exchange rate at the coalescence temperature is given by  $K_{ex} = \pi\Delta\nu/\sqrt{2}$ . See: Günther, H. *NMR Spectroscopy*; John Wiley: Chichester, U.K., 1980; p 243.

**Scheme 4.** Representation of the Rearrangement Proposed to Occur for Compounds 6, 7, and 10 in Solution

relaxation exhibit the opposite phase. Figure 2 shows the EXSY spectrum of 6 recorded at 230 K using a mixing time of 2.5 s. Below, the rows crossing the diagonal at 5.54 ppm (H<sup>1</sup>) and 3.87 ppm (H<sup>4</sup>) are shown. Similar spectra were obtained for compounds 8 to 10 but not for the trimolybdenum complex 7, which will be discussed later. Inspection of the cross peaks in the spectrum of 6 clearly indicate that H<sup>1</sup> and H<sup>4</sup> do experience mutual exchange. As expected, transfer of magnetization is more efficient (more intense cross peak) from H<sup>4</sup> to H<sup>1</sup> than the reverse, because the latter relax more slowly. On the other hand, the stronger positive peaks reveal the spatial proximity between, for example, H<sup>4</sup> and Cp<sup>1</sup> or H<sup>3</sup>. However, there are also weaker positive cross peaks (in that case, at the Cp<sup>2</sup> and H<sup>2</sup> positions), which are indirectly derived from the chemical exchange H<sup>4</sup>/H<sup>1</sup>. This is confirmed by the fact that the intensity of these "secondary" peaks increases at higher temperatures, when chemical exchange is faster. Finally, when using mixing times short with respect to the relaxation rates (for example, 0.4 s), all positive peaks practically disappear, as expected for cross peaks arising from cross relaxation,<sup>26</sup> but chemical exchange is still fast enough so as to give strong negative off-diagonal peaks.

Having firmly established the chemical exchanges occurring in our trimetal species, a reasonable mechanism is to be proposed. In first place, we can safely exclude any mechanism involving dissociation of the cyclopentadienyldiene moieties (CO)<sub>3</sub>M(C<sub>5</sub>H<sub>4</sub>). This is based on the observation that a 2D EXSY spectrum of a mixture of compounds 8, 9, and 10 showed no cross peaks which would relate resonances belonging to different compounds. Should such a dissociation take place, both 8 and 10 would generate the same metal fragment [(CO)<sub>3</sub>Mo(C<sub>5</sub>H<sub>4</sub>)], and, therefore, cross peaks between the H<sub>1</sub>/H<sub>4</sub> resonances of 8 and those of 10 should be observed. Then we conclude that any processes responsible for the observed exchanges must be intramolecular. Moreover, in spite of the fact that the estimated activation energies in complexes 6, 7, and 10 are virtually identical for both the H<sup>2</sup>/H<sup>3</sup> and Cp<sup>1</sup>/Cp<sup>2</sup> exchanges, we believe they arise from different fluxional processes, which accidentally have about the same activation energy (Schemes 3 and 4).

The first process would be operative in all complexes 6 to 10. It is supposed to involve rotation of the (CO)<sub>3</sub>M(C<sub>5</sub>H<sub>4</sub>) moiety around a vector joining the central metal atom and the midpoint of the M–C(10) bond (Scheme 3), which must be

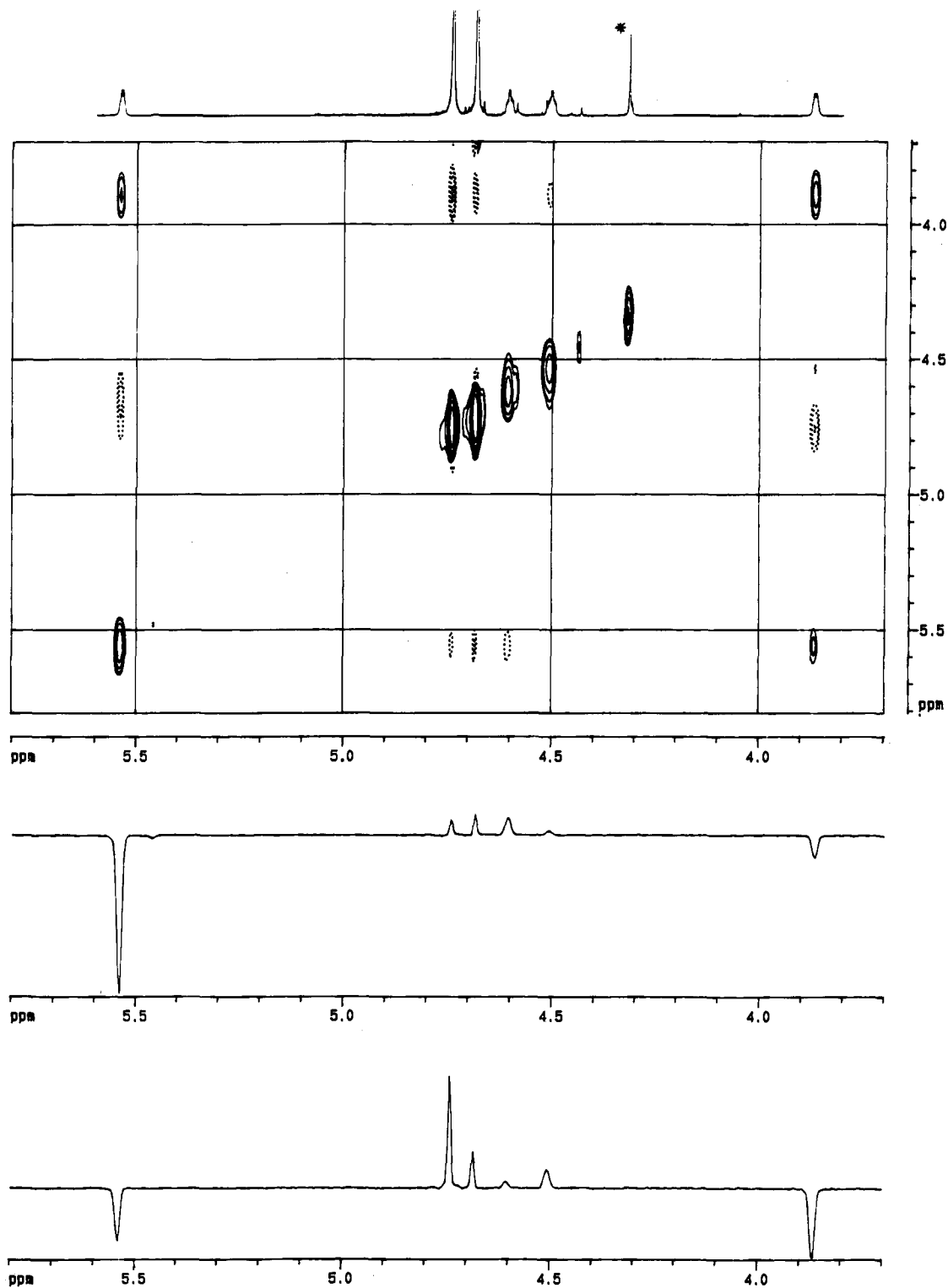


**Figure 2.** Contour plot of the  $^1\text{H}$  phase-sensitive 2D EXSY spectrum of compound **6** (toluene- $d_8$ , 230 K, mixing time 2.5 s). A total of 8 transients of 2 K data points were collected over a spectral width of 3150 Hz for 128 increments in  $D_0$ . Zero-filling in  $F_1$  and weighting functions in both dimensions were applied before transformation. Positive peaks are represented by dotted lines and negative peaks by normal lines. The spectrum on the top is the 1D  $^1\text{H}$  spectrum of the complex (the peak marked with an asterisk corresponds to an impurity). Below the contour plot, the rows of the 2D spectrum crossing the diagonal line at 5.54 and 3.87 ppm, respectively, are shown.

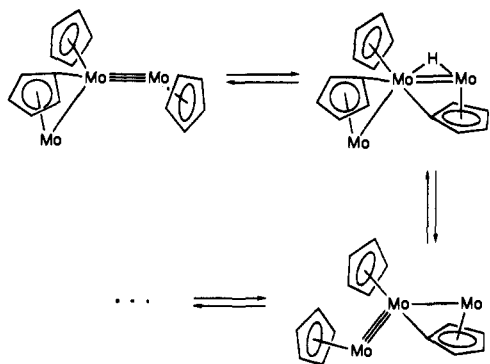
accompanied by mutual exchange between the semibridging carbonyls ( $\text{C}^1$  and  $\text{C}^2$ ). The latter is known to be a low-energy process, requiring an activation of *ca.* 45  $\text{kJmol}^{-1}$ , as deduced from studies on the triply bonded species  $[\text{MoWCp}_2(\text{CO})_4]^{28}$  and  $[\text{Mo}_2\text{Cp}_2(\text{CO})_3\text{L}]$ , ( $\text{L} = \text{PhP}(\text{OCH}_2\text{CH}_2)_2\text{NH}$ ).<sup>29</sup> Then, except for the trimolybdenum complex **7**, the measured activation energy of *ca.* 62  $\text{kJmol}^{-1}$  must be due mostly to the rotation

of the  $(\text{CO})_3\text{M}(\text{C}_5\text{H}_4)$  moiety. In that case, it is perhaps not surprising that all measured activation energies (except for **7**) are so similar, as they all involve a rotating cyclopentadi-

(28) Curtis, M. D.; Fotinos, N. A.; Messerle, L.; Sattelberger, A. P. *Inorg. Chem.* **1983**, *22*, 1559–1561.

(29) Wachter, J.; Riess, J. G.; Mitschler, A. *Organometallics* **1984**, *3*, 714–722.

**Scheme 5.** Oversimplified Representation of the Rearrangements Proposed in Order to Explain the  $C_5H_5/C_5H_4$  Exchange in the Solutions of Compound **7** (carbonyl ligands omitted for clarity)



enylidene group  $\sigma$ -bonded to the same metal moiety (the central tungsten atom), and this rotation is expected to weaken (or break) this bonding interaction in the transient stage. Moreover, this is consistent with the much lower barrier measured for the trimolybdenum compound **7** (*ca.* 47 kJmol<sup>-1</sup>). Indeed, the low thermal stability of this species must be due in great part to a lower strength of the cyclopentadienylidene  $\sigma$ -bond to the central molybdenum atom (compared to tungsten).

In a broad sense, the proposed rotation of the  $(CO)_3M(C_5H_4)$  moiety in compounds **6** to **10** resembles that of alkenes bonded to transition metal fragments. It is perhaps a coincidence that the energy barrier for rotation found in our complexes (when the central atom is tungsten) is very similar to those determined for the rotation of  $C_2H_4$  in the mononuclear tungsten complexes  $[W(CH_3)(\eta^2-C_2H_4)(CO)_3L]$  ( $\Delta G^\ddagger = 60.1$  and 62.7 kJmol<sup>-1</sup> for  $L = Cp$  and indenyl, respectively).<sup>30</sup>

Although the rearrangement just discussed provides a satisfactory explanation for the chemical exchange observed for the cyclopentadienylidene ligand in the trimetal species **6** to **10**, it cannot account for the coalescence of the cyclopentadienyl resonances in compounds **6**, **7**, and **10** (those species containing a homometallic triple bond). To explain the latter, it is necessary to invoke a migration of the  $(CO)_3M(C_5H_4)$  group across the triple bond (Scheme 4). This has to be counterbalanced by migration of the carbonyl ligand occupying a related coordination position ( $C^6$ ), possibly through a triangular core structure (**A** in Scheme 4). We recall here that the energy difference between open and triangular metal cores in 46-electron clusters may be small (Chart 1). A final exchange between the semibridging carbonyls ( $C^1$  and  $C^2$ ), as proposed for the rotation rearrangement, completes the exchange between the chemical environments of  $Cp^1$  and  $Cp^2$ . It is worth noting here that the 46-electron trimetal complex  $[FeMoCp_2\{\mu-PhPC_6H_4PPh\}(CO)_5]$ , which has the same type of structure as our compounds, also experiences a dynamic process equalizing the chemical environments of the metal atoms linked by the triple bond.<sup>24</sup> Finally, it should be noted that the rearrangement just proposed also accounts for the  $H_2/H_3$  exchange.

The previous proposal would itself explain all observations in the case of compounds **6**, **7**, and **10**. However, it has to be excluded in the case of compounds **8** and **9**, as it would represent an unfavorable isomerization (the  $C_5H_4$  ligand would become  $\sigma$ -bonded to molybdenum), rather than a fluxional rearrangement. On the other hand, there is no reason why the rotation mechanism should be excluded in the former compounds. Then,

we are forced to admit the occurrence of two independent processes, one operating in all complexes (Scheme 3), and the other (Scheme 4) operating only in the complexes having a homometallic triple bond (**6**, **7**, and **10**). Therefore, the fact that the estimated energy barriers for both of them are virtually identical has to be regarded as accidental. As both processes account for the  $H_2/H_3$  exchange but only one of them does for the  $Cp^1/Cp^2$  exchange, it should be expected that the former exchange is faster than the later one. Unfortunately, the broadness of the  $H_2/H_3$  resonances in our compounds near coalescence precludes very precise measurements of the coalescence temperatures. This, added to the noticeable changes in all chemical shifts with temperature, introduces substantial uncertainty in the estimation of the exchange rates at the coalescence temperature.<sup>27</sup> In spite of this, taking our more precise data (those from **6**), we can estimate  $K^{297} = ca. 90 s^{-1}$  for the  $H_2/H_3$  exchange and  $K^{297} = ca. 60 s^{-1}$  for the  $Cp^1/Cp^2$  exchange, in agreement with the above predictions.

As we have mentioned above, the 2D EXSY spectrum of the trimolybdenum species **7** (Figure 3) shows important differences when compared with those from the other trimetal compounds (Figure 2). From that spectrum, it can be seen that either  $H^1$  or  $H^4$  is related to all other protons in the molecule ( $C_5H_4$  and  $Cp$  ligands) by chemical exchange rather than by cross relaxation. The relevant off-diagonal peaks (4.59, 4.52, 4.42, and 4.23 ppm) behave as expected<sup>31</sup> for peaks due to a process taking place at a rate slower than those previously discussed. Their intensities increase more rapidly than those due to the  $H^1/H^4$  mutual exchange as we increase the mixing time from 0.4 to 3 s in the EXSY experiment. This increase in negative intensity occurs in spite of the fact that at the longer mixing time a substantial positive intensity contribution must develop in these off-diagonal peaks, due to cross relaxation (*cf.* Figure 2). Thus, we trust we are facing a genuine exchange process which, when combined with the ones previously discussed, effectively accomplishes a general scrambling of all protons in the molecule. Unfortunately, the extensive decomposition of **7** above  $-20^\circ C$  precludes a more direct observation of this new exchange process. In spite of this, the data just discussed provide a strong piece of evidence for the reversible interconversion between  $C_5H_4$  and  $C_5H_5$  ligands in complex **7**. To our knowledge, this sort of exchange process has been never reported previously. However, taking into account that the oxidative additions of C-H bonds in cyclopentadienyl ligands can be reversible,<sup>5</sup> it is not unreasonable to suppose that the  $C_5H_4/C_5H_5$  exchange in **7** could take place through a combination of several C-H oxidative addition/reductive elimination steps (Scheme 5, oversimplified view). Moreover, we note that similar steps have been previously proposed in order to explain the proton exchange between cyclopentadienyl and tetrahydroborate<sup>32</sup> or hydrido ligands.<sup>16g,33</sup>

**New Reaction Pathways for the Photolytic Decarbonylation of the  $[M_2Cp_2(CO)_6]$  Dimers ( $M = Mo, W$ ).** The previously established photochemistry of the group 6 dimers  $[M_2Cp_2(CO)_6]$  (see Introduction and Scheme 2) cannot explain the formation of the trimetal compounds **6** to **10**. In order to achieve this, it has to be assumed that a new reaction pathway generating cyclopentadienylidene ligands operates in the system. Our proposal for the latter (Scheme 6) is based on our previous findings on the dppm-bridged ditungsten system (Scheme 1).<sup>5</sup>

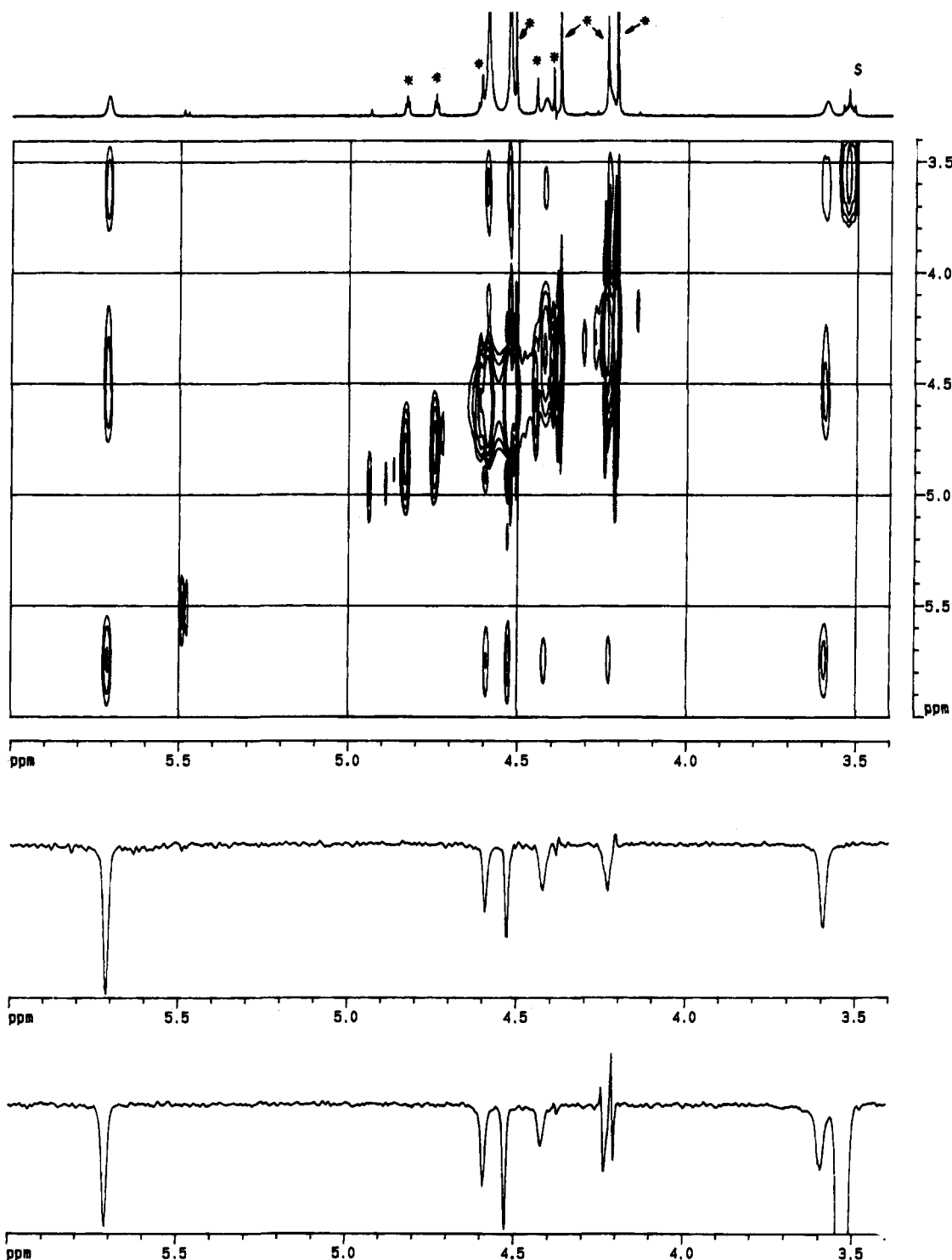
(31) Gielen, M.; Willem, R. In *Topics in Physical Organometallic Chemistry*, Vol. 2; Gielen, M. F., Ed.; Freund Publishing House: London, U.K., 1988; p 165.

(32) Marks, T. J.; Kolb, J. R. *J. Am. Chem. Soc.* **1975**, *97*, 3397-3401.

(33) Alcock, N. W.; Howarth, O. W.; Moore, P.; Morris, G. E. *J. Chem. Soc., Chem. Commun.* **1979**, 1160-1162.

(30) Kreiter, C. G.; Kurt, N.; Alt, H. G. *Chem. Ber.* **1981**, *114*, 1845-1852.



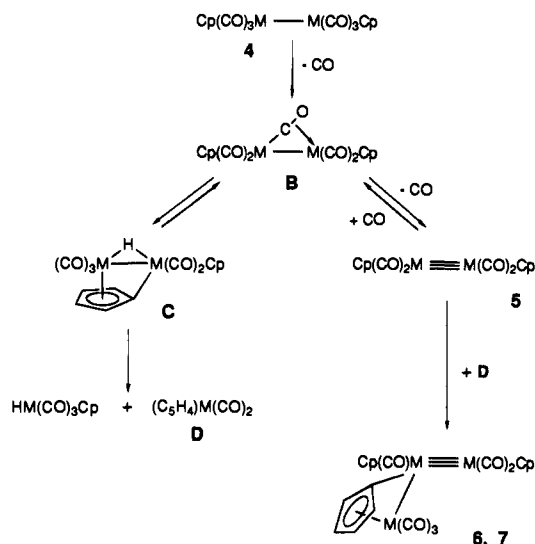


**Figure 3.** Contour plot of the  $^1\text{H}$  phase-sensitive 2D EXSY spectrum of compound **7** (toluene- $d_8$ , 193 K, mixing time 3 s). A total of 24 transients of 2 K data points were collected over a spectral width of 3150 Hz for 64 increments in D0. Processing and plotting of the data were carried out as described in Figure 2. Peaks marked with an asterisk in the 1D spectrum on the top correspond to impurities generated during sample preparation, and that marked with an "S" corresponds to residual tetrahydrofuran in the solution. The rows shown below cross the diagonal of the 2D spectrum at 5.71 and 3.59 ppm, respectively.

We assume that the primary photoproduct **B** experiences two different processes: (a) further decarbonylation to yield the triply bonded dimers **5**, as previously established by other authors (Scheme 2) and (b) intramolecular oxidative addition of a C–H (cyclopentadienyl) bond, to yield a hydrido cyclopentadienylidene intermediate **C**. The relative efficiencies of these two pathways is likely to be strongly dependent on experimental conditions (temperature, rate of flow of the nitrogen purge, etc.). Under the conditions employed by us, both pathways seem to

be similarly efficient, as judged from spectroscopic monitoring of the reaction mixtures. On the other hand, the isomerization **B** to **C** is completely analogous to that observed for  $[\text{W}_2\text{Cp}_2(\mu-\eta^1, \eta^2\text{-CN}^t\text{Bu})(\text{CO})_2(\mu\text{-dppm})]$ , which spontaneously transforms into  $[\text{W}_2(\mu\text{-H})(\mu-\eta^1, \eta^5\text{-C}_5\text{H}_4)\text{Cp}(\text{CO})_2(\text{CN}^t\text{Bu})(\mu\text{-dppm})]$  at room temperature.<sup>5</sup>

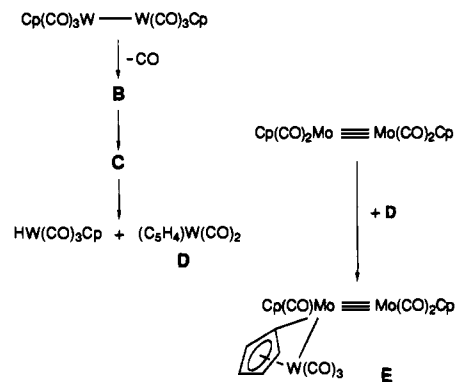
Intermediate **C**, possibly because the lack of an efficient binucleating ligand (as the dppm ligand is), breaks down rapidly to yield the corresponding mononuclear hydride  $[\text{MH}(\text{CO})_3\text{Cp}]$

**Scheme 6.** Reaction Pathways Proposed for the Formation of Trinuclear Species During the Photolysis of  $[M_2Cp_2(CO)_6]$  Dimers ( $M = Mo, W$ )

and a highly reactive cyclopentadienylidene metal fragment **D**. The mononuclear hydrides are actually isolated from the reaction mixtures, although their relative amounts decrease with reaction time, as they transform into the dinuclear species  $[W_2(\mu-H)_2Cp_2(CO)_4]$  or  $[Mo_2Cp_2(CO)_4]$ , respectively, in agreement with previous photochemical studies on these hydrido complexes.<sup>18</sup> Finally, the highly unsaturated fragments **D** would rapidly react with the triply bonded dimers **5** to yield the trimetallic species **6** or **7**, after some rearrangement of the carbonyl ligands.

The pathways just proposed justify the products isolated in our photochemical experiments on the dimers  $[M_2Cp_2(CO)_6]$  ( $M = Mo, W$ ), although we have no direct evidence for the formation of the mononuclear cyclopentadienylidene intermediate **D**. However, if our hypothesis were to be correct at a reasonable extent, we would expect to favor the formation of a dimolybdenum–tungsten complex analogous to the homometallics **6** or **7** upon photolysis of equimolar amounts of  $[W_2Cp_2(CO)_6]$  and  $[Mo_2Cp_2(CO)_4]$  (Scheme 7). Indeed, this reaction yields the dimolybdenum–tungsten complex **8** as major trimetallic species, while  $[WH(CO)_3Cp]$  and  $[W_2(\mu-H)_2Cp_2(CO)_4]$  are the major hydrido species formed. However, the structure of **8** differs from the expected one (**E** in Scheme 7) in that the central atom is tungsten instead of molybdenum, and the cyclopentadienylidene ligand is found  $\sigma$ -bonded to tungsten rather than to a molybdenum atom. As we have noted above, we regard this as the result of a marked thermodynamic preference for the  $C_5H_4$  ligand to be  $\sigma$ -bonded to tungsten. Thus, it is possible that **E** is actually formed as a primary product, but then experiences rapidly an isomerization process to give the more stable species **8**. This could be accomplished through C–H oxidative addition/reductive elimination steps involving the  $C_5H_5$  and  $C_5H_4$  ligands, in a similar way to that proposed to occur in solution for complex **7** (Scheme 5).

On the other hand, the formation in lower yields of the trinuclear species **6**, **9**, and **10** can be understood along the same lines. Even in the presence of  $[Mo_2Cp_2(CO)_4]$ , the normal decarbonylation products of  $[W_2Cp_2(CO)_6]$  should be obtained, although in lower yields. Thus, the formation of minor amounts of **6** is explained. In addition, this also implies that some  $[W_2Cp_2(CO)_4]$  must be present in the reaction mixture. On the other hand, some CO must be obviously available during the photolysis, which allows the dimolybdenum reagent **5** to generate some pentacarbonylic intermediate **C**, which in turn

**Scheme 7.** Dominant Processes Thought to Occur During the Photolysis of Equimolar Mixtures of  $[W_2Cp_2(CO)_6]$  and  $[Mo_2Cp_2(CO)_4]$ 

would give **7** (trace amounts detected) or ditungsten–molybdenum species, after reaction of the corresponding mononuclear fragment **D** ( $M = Mo$ ) with  $[W_2Cp_2(CO)_4]$ . The latter reaction should give selectively complex **10** ( $Mo-W\equiv W$  skeleton), but, in fact, we obtain this species along with **9** ( $W-W\equiv Mo$  skeleton), in relative amounts depending somewhat on experimental conditions. Therefore, it is not unreasonable to assume that an isomerization (**10** to **9**) takes place at some extent during photolysis. This isomerization would be similar to that thought to occur for the dimolybdenum–tungsten species (**E** to **8**; see also Scheme 5). In fact, when performing the photolysis for longer periods of time, the ratio **9**:**10** in the final mixture increased noticeably. However, this also caused extensive decomposition in the overall mixture, so no clear conclusions can be drawn out of these observations.

**Note on the Thermal Decarbonylations of Dimers  $[M_2Cp_2(CO)_6]$  ( $M = Mo, W$ ).** Thermal decarbonylation of the dimers  $[M_2Cp_2(CO)_6]$  ( $M = Mo, W$ ) in a high boiling point solvent is a well-established and efficient method for the synthesis of the triply bonded complexes  $[M_2Cp_2(CO)_4]$ .<sup>28</sup> Taking into account the low or moderate thermal stability of the trinuclear complexes **7** or **6**, it is clear that there is no chance they could be detected as products in the above high-temperature reactions, were they formed at all. However, when preparing the ditungsten tetracarbonyl complex by the above method (in refluxing diglyme solution), we have always detected (by IR spectroscopy) the presence of small amounts of  $[WH(CO)_3Cp]$  in the resulting solution. While this is irrelevant concerning the synthetic method, it suggests that the C–H cleavages occurring in the photochemical decarbonylation of dimers  $[M_2Cp_2(CO)_6]$  might be also operative in the corresponding thermal reactions, although they do not lead to appreciable amounts of products.

## Conclusions

The results here reported show for the first time that the low-temperature photolysis of the dimers  $[M_2Cp_2(CO)_6]$  ( $M = Mo, W$ ) in solution generates, *inter alia*, intermediate species which act as sources of  $[MH(CO)_3Cp]$  and the cyclopentadienylidene metal fragment  $[M(C_5H_4)(CO)_2]$ . The latter is “trapped” in the form of the new trinuclear species  $[M_3(\mu-\eta^1, \eta^5-C_5H_4)Cp_2(CO)_6]$ . It is proposed that both mononuclear moieties arise from the fragmentation of  $[M_2(\mu-H)(\mu-\eta^1, \eta^5-C_5H_4)Cp(CO)_5]$ , which in turn would result from an intramolecular oxidative addition of a C–H (cyclopentadienyl) bond in the primary photoproduct  $[M_2Cp_2(\mu-\eta^1, \eta^5-CO)(CO)_4]$ . This hypothesis is also consistent with the formation of the heterometallic complexes  $[Mo_2W(\mu-\eta^1, \eta^5-C_5H_4)Cp_2(CO)_6]$  and  $[MoW_2(\mu-\eta^1, \eta^5-C_5H_4)Cp_2(CO)_6]$  in

the photolysis of equimolar amounts of  $[\text{W}_2\text{Cp}_2(\text{CO})_6]$  and  $[\text{Mo}_2\text{Cp}_2(\text{CO})_4]$ . The cyclopentadienyldiene ligand in the new trinuclear compounds exhibits a marked preference (presumably thermodynamic) to form  $\sigma$  bonds to tungsten rather than to molybdenum atoms, as judged from the structure, thermal stability, and dynamic behavior of these species. Moreover, when bonded through a relatively weak  $\sigma$  bond to molybdenum, the cyclopentadienyldiene ligand experiences a full proton exchange with the cyclopentadienyl groups of the molecule, as revealed by 2D EXSY experiments on the trimolybdenum compound  $[\text{Mo}_3(\mu-\eta^1, \eta^5\text{-C}_5\text{H}_4)\text{Cp}_2(\text{CO})_6]$ .

## Experimental Section

**General Comments.** All manipulations and reactions were carried out under a nitrogen (99.9995%) atmosphere, using standard Schlenk techniques. Solvents were purified according to literature procedures<sup>34</sup> and distilled prior to use. Petroleum ether refers to that fraction distilling in the range 65–70 °C. The complexes  $[\text{M}_2\text{Cp}_2(\text{CO})_6]$  (M = Mo, W)<sup>35</sup> and  $[\text{Mo}_2\text{Cp}_2(\text{CO})_4]$ <sup>28</sup> were prepared as described previously. Photochemical experiments were performed using jacketed Pyrex Schlenk tubes, refrigerated by a closed 2-propanol circuit kept at the desired temperature with a cryostat. A 400-W mercury lamp (Applied Photophysics), placed *ca.* 1 cm away from the Schlenk tube, was used for these experiments. Low-temperature chromatographic separations were carried out analogously using jacketed columns. Commercial Florisil (Aldrich, 100–200 mesh) and aluminum oxide (Aldrich, Activity I, 150 mesh) were degassed under vacuum prior to use. The later was afterwards mixed under nitrogen with the appropriate amount of water to reach the activity desired.

**NMR Measurements.** NMR spectra on degassed solutions of complexes **6** to **10** were routinely recorded at 300.13 MHz (<sup>1</sup>H) or 75.47 MHz (<sup>13</sup>C{<sup>1</sup>H}). High-temperature <sup>1</sup>H spectra of compounds **6** and **8** were measured at 200.13 MHz. 2D EXSY experiments were carried out at 400.13 MHz and were performed in the phase-sensitive mode in order to detect both exchange and cross-relaxation phenomena. The usual pulse sequence (D1– $\pi/2$ –D0– $\pi/2$ – $\tau_m$ – $\pi/2$ –adqu) was used for this purpose (D1 = relaxation delay = 1.5 s; D0 = 2D incremental delay;  $\tau_m$  = mixing time).<sup>26,36</sup> At least two experiments were carried out for each complex, using different mixing times, usually in the range 0.4–3 s. Generally, the use of the shorter mixing time was enough to suppress almost completely all off-diagonal peaks due to cross relaxation. In the case of complex **6**, 2D spectra were also recorded at different temperatures (295 K and 230 K), and  $T_1$  for all resonances were measured at 230 K by the inversion-recovery method.<sup>26</sup> The values given by the routine of the spectrometer were  $H^1 = 2.4$  s;  $H^2 = 1.8$  s;  $H^3 = 1.7$  s;  $H^4 = 0.8$  s;  $\text{Cp}^1 = 1.4$  s;  $\text{Cp}^2 = 6.6$  s (see Table 4 for labeling scheme).

**Photolysis of  $[\text{W}_2\text{Cp}_2(\text{CO})_6]$ .** A toluene solution (20 mL) of the title compound (0.066 g, 0.1 mmol) was irradiated at –35 °C for 3 h while bubbling nitrogen gently through the solution. Solvent was then removed under vacuum from the brown mixture obtained, and the residue was chromatographed on an alumina column (Activity III, 30 × 2.5 cm) at –35 °C. Elution with toluene:petroleum ether (1:1) gave an orange–brown fraction containing the complexes  $[\text{WH}(\text{CO})_3\text{Cp}]$  and  $[\text{W}_2(\mu\text{-H})_2(\text{CO})_4\text{Cp}_2]$ , along with a small amount of  $[\text{W}_2\text{Cp}_2(\text{CO})_4]$ . Elution with toluene gave a brown fraction. Removal of the solvent under vacuum from the latter yielded  $[\text{W}_3(\mu-\eta^1, \eta^5\text{-C}_5\text{H}_4)\text{Cp}_2(\text{CO})_6]$  (**6**) as a brown microcrystalline solid (0.032 g, 0.035 mmol, 70%). The black crystals used in the X-ray study were grown from a solution of **6** in a dichloromethane/toluene/petroleum ether mixture, at –20 °C. Anal. Calcd for  $\text{C}_{21}\text{H}_{14}\text{O}_6\text{W}_3$ , **6**: C, 27.58; H, 1.55. Found: C, 27.85; H, 1.65.

**Photolysis of  $[\text{Mo}_2\text{Cp}_2(\text{CO})_4]$ .** A toluene solution (20 mL) of the title compound (0.100 g, 0.20 mmol) was irradiated at –35 °C for 2 h

while bubbling nitrogen through the solution gently. The mixture was then chromatographed on a Florisil column (30 × 2.5 cm) at –25 °C. Elution with toluene/petroleum ether (1:1) gave an orange fraction containing  $[\text{MoH}(\text{CO})_3\text{Cp}]$  and  $[\text{Mo}_2\text{Cp}_2(\text{CO})_4]$ . Elution with toluene gave a brown fraction which was collected at –25 °C. Removal of solvent from the latter at the same temperature yielded essentially pure  $[\text{Mo}_3(\mu-\eta^1, \eta^5\text{-C}_5\text{H}_4)\text{Cp}_2(\text{CO})_6]$  (**7**), as a brown solid. This complex is thermally unstable at room temperature and is also very air-sensitive. Therefore, satisfactory microanalytical data could not be obtained. <sup>1</sup>H NMR spectra of **7** always showed variable amounts of decomposition products generated during sample preparation.

**Photolysis of Equimolar Mixtures of  $[\text{W}_2\text{Cp}_2(\text{CO})_6]$  and  $[\text{Mo}_2\text{Cp}_2(\text{CO})_4]$ .** In a typical experiment, a toluene solution (40 mL) containing  $[\text{Mo}_2\text{Cp}_2(\text{CO})_4]$  (0.100 g, 0.23 mmol) and  $[\text{W}_2\text{Cp}_2(\text{CO})_6]$  (0.153 g, 0.23 mmol) was irradiated at –35 °C for 2.5 h while bubbling nitrogen through the solution gently. The mixture was then chromatographed on a Florisil column (40 × 2.5 cm) at –30 °C. Elution with toluene gave an orange fraction containing  $[\text{WH}(\text{CO})_3\text{Cp}]$ ,  $[\text{W}_2(\mu\text{-H})_2(\text{CO})_4\text{Cp}_2]$ ,  $[\text{Mo}_2\text{Cp}_2(\text{CO})_4]$ , and trace amounts of  $[\text{MoH}(\text{CO})_3\text{Cp}]$ . Elution with tetrahydrofuran/petroleum ether (1:9) gave a very broad red–brown band immediately followed by an orange–brown one. Removal of solvent from the latter yielded almost pure compound **6** (0.010 g, 0.011 mmol, 10% based on W). The red–brown fraction was chromatographed again on Florisil at –30 °C using a tetrahydrofuran/petroleum ether (1:15) mixture as eluant. Two ill-differentiated bands, having about the same color, were collected separately. The first fraction was shown (by <sup>1</sup>H NMR) to contain essentially pure  $[\text{Mo}_2\text{W}(\mu-\eta^1, \eta^5\text{-C}_5\text{H}_4)\text{Cp}_2(\text{CO})_6]$  (**8**), which could be isolated as a brown microcrystalline solid by removal of solvents under vacuum (0.040 g, 0.054 mmol, 24% based on Mo). The black crystals used in the X-ray study were grown from a solution of **8** in a toluene/petroleum ether mixture, at –20 °C. Anal. Calcd for  $\text{C}_{21}\text{H}_{14}\text{O}_6\text{Mo}_2\text{W}$ , **8**: C, 34.15; H, 1.92. Found: C, 34.37; H, 1.77. Removal of solvents under vacuum from the second fraction afforded a brown microcrystalline solid shown (by <sup>1</sup>H NMR) to contain a mixture of two isomers of formula  $[\text{MoW}_2(\mu-\eta^1, \eta^5\text{-C}_5\text{H}_4)\text{Cp}_2(\text{CO})_6]$  (**9**, **10**), in similar relative amounts (overall yield 0.020 g, 0.024 mmol, 11% based on W). The exact ratio **9**:**10**, however, was found to depend on experimental conditions. All attempts to separate **9** from **10** were unsuccessful. Moreover, crystallization of the usual mixture from toluene/petroleum ether at –20 °C yielded black single crystals shown to have the composition 0.5 **9** + 0.5 **10**. Anal. Calcd for  $\text{C}_{21}\text{H}_{14}\text{O}_6\text{MoW}_2$ , (**9** or **10**): C, 30.52; H, 1.71. Found: C, 30.85; H, 1.60.

**X-ray Data Collection, Structure Determination and Refinements for Compounds **6**, **8**, and **9**:**10**.** Unit cell dimensions with estimated standard deviations were obtained from least-squares refinements of the setting angles of 25 well-centered reflections. Two standard reflections were monitored every 2 h; they showed no change during data collection except for compound **6**, which experienced a 30% intensity decay over the period of the experiment. In that case, a correction was applied. Crystallographic data and other pertinent information are summarized in Table 1. Corrections were made for Lorentz and polarization effects. Empirical absorption corrections (Difabs)<sup>37</sup> were applied.

Computations were performed by using CRYSTALS<sup>38</sup> adapted on a Micro Vax II. Atomic form factors for neutral C, O, Mo, W, and H were taken from ref 39. Anomalous dispersion was taken into account. The structures were solved by direct methods and subsequent Fourier maps. Not all hydrogen atoms could be found on difference maps for compounds **6** and **8**, so they were all theoretically located in these cases. In all cases hydrogen atoms were given an isotropic overall thermal parameter, but nonhydrogen atoms were anisotropically refined. Least-squares refinements were carried out with approximation in three blocks to the normal matrix by minimizing the function  $\sum w(|F_o| - |F_c|)^2$  where

(37) Walker, N.; Stuart, D. *Acta Crystallogr., Sect. A* **1983**, *39*, 158–166.

(38) Watkin, D. J.; Carruthers, J. R.; Betteridge, P. W. *CRYSTALS*. An Advanced Crystallographic Program System; Chemical Crystallography Laboratory, University of Oxford: Oxford, U.K., 1988.

(39) *International Tables for X-Ray Crystallography*; Kynoch Press: Birmingham, U.K., 1974; Vol. IV.

(34) Perrin, D. D.; Armarego, W. L. F. *Purification of Laboratory Chemicals*; Pergamon Press: Oxford, U.K., 1988.

(35) Birdwhistell, R.; Hackett, P.; Manning, R. J. *Organomet. Chem.* **1978**, *257*, 239–241.

(36) Orrell, K. G.; Sik, V. *Annu. Rep. N.M.R. Spectrosc.* **1987**, *18*, 79–173.

$F_o$  and  $F_c$  are the observed and calculated structure factors. Unit weight was used. Models reached convergence with  $R = \sum(|F_o| - |F_c|)/\sum|F_o|$  and  $R_w = [\sum w(|F_o| - |F_c|)^2/\sum w(F_o)^2]^{1/2}$  having values listed in Table 1. Criteria for satisfactory complete analysis were the ratios of root-mean-square shifts to standard deviation being less than 0.1 and no significant features in the final difference map. Figure 1 shows a view of the molecular structure of the molybdenum-ditungsten complex using CAMERON.<sup>40</sup> In that case, the cluster contains a central tungsten atom, to which the cyclopentadienylidene ligand is  $\sigma$ -linked. However, the two other metal positions were statistically occupied by W and Mo, and have been labeled X(1) and X(2) in Figure 1. Therefore, two plausible crystallographic descriptions are possible: (a) a crystal containing an equimolar mixture of compounds **6** (W-W≡W skeleton) and **8** (Mo-W≡Mo skeleton) or (b) a mixture of isomers **9** (W-W≡Mo) and **10** (Mo-W≡W). The latter proved to be the case, as shown by the <sup>1</sup>H NMR spectrum of the crystals used. In any case, refinements were independent of the particular choice and were carried out locating

(40) Pearce, L. J.; Watkin, D. J. Chemical Crystallography Laboratory, University of Oxford, U.K.

on each site [X(1) and X(2)] molybdenum and tungsten atoms with an occupancy factor of 0.5.

**Acknowledgment.** We thank the DGICYT of Spain for financial support (Project PB91-0678) and the FICYT of Asturias (Spain) for a grant to M. A. Alvarez.

**Supplementary Material Available:** CAMERON diagrams of the molecular structure for compounds **6** and **8** (Figures S1 and S2) and a listing of atomic coordinates for nonhydrogen atoms (Tables S1–S3), for hydrogen atoms (Tables S4–S6), anisotropic thermal parameters (Tables S7–S9), and interatomic distances and angles (Tables S10–S12) for the three structure determinations (12 pages). This material is contained in many libraries on microfiche, immediately follows this article in the microfiche edition, and can be ordered from the ACS; see any current masthead page for ordering information. Tables of observed and calculated structure factors may be also obtained from the authors on request.

JA942891E